

Multiple autophosphorylation sites are dispensable for murine ATM activation in vivo

Jeremy A. Daniel,¹ Manuela Pellegrini,^{1,2} Ji-Hoon Lee,³ Tanya T. Paull,³ Lionel Feigenbaum,⁴ and André Nussenzweig¹

¹Experimental Immunology Branch, National Cancer Institute, National Institutes of Health, Bethesda, MD 20892

²Department of Public Health and Cellular Biology, University of Tor Vergata, 00175 Rome, Italy

³Department of Molecular Genetics and Microbiology, Institute of Cellular and Molecular Biology, University of Texas at Austin, Austin, TX 78712

⁴Science Applications International Corporation–Frederick, National Cancer Institute at Frederick Cancer Research and Development Center, Frederick, MD 21702

Cellular responses to both physiological and pathological DNA double-strand breaks are initiated through activation of the evolutionarily conserved ataxia telangiectasia mutated (ATM) kinase. Upon DNA damage, an activation mechanism involving autophosphorylation has been reported to allow ATM to phosphorylate downstream targets important for cell cycle checkpoints and DNA repair. In humans, serine residues 367, 1893, and 1981 have been shown to be autophosphorylation sites that are individually required for ATM activation. To test the physiological importance of these sites, we generated

a transgenic mouse model in which all three conserved ATM serine autophosphorylation sites (S367/1899/1987) have been replaced with alanine. In this study, we show that ATM-dependent responses at both cellular and organismal levels are functional in mice that express a triple serine mutant form of ATM as their sole ATM species. These results lend further support to the notion that ATM autophosphorylation correlates with the DNA damage-induced activation of the kinase but is not required for ATM function in vivo.

Introduction

Double-strand breaks (DSBs) in DNA can occur from chemical damage or γ irradiation as well as during normal physiological processes, including antigen receptor gene rearrangement and meiosis. Unrepaired DSBs are a source of genomic instability that can lead to uncontrolled cell proliferation and cancer (McKinnon and Caldecott, 2007). After sensor proteins recognize damaged chromatin, the ataxia telangiectasia mutated (ATM) kinase is recruited to the break site and initiates a cellular response through phosphorylation of consensus sites on numerous substrates that signal for repair of the DNA and/or prevent cell cycle progression (Shiloh, 2003). In addition to amplifying the DNA damage signal, ATM may also participate more directly in DNA repair by stabilizing repair complexes on damaged chromatin (Bredemeyer et al., 2006). The critical function of ATM in maintaining genomic stability is underscored by its high conservation in eukaryotes and its deficiency in the cancer-prone ataxia telangiectasia disease (Shiloh, 2003).

ATM kinase activity is directly stimulated by damaged DNA and the MRE11–RAD50–NBS1 (MRN) sensor complex, which also stabilizes ATM to the break site (Girard et al., 2002; Carson et al., 2003; Uziel et al., 2003; Lee and Paull, 2004, 2005; Difilippantonio et al., 2005; Cerosaletti et al., 2006; Dupre et al., 2006; Berkovich et al., 2007; You et al., 2007). The DNA damage-induced activation of ATM results in the dissociation of inactive ATM dimers and/or multimers into enzymatically active monomers (Bakkenist and Kastan, 2003; Lee and Paull, 2004; Dupre et al., 2006). An autophosphorylation mechanism has been proposed to initiate ATM activation upon DNA damage by promoting monomerization and subsequent localization of ATM to break sites (Bakkenist and Kastan, 2003; Berkovich et al., 2007). In human cells, serine residues 367, 1893, and 1981 (S367, S1893, and S1981) have been shown to be autophosphorylation sites that are individually required for ATM activation and function (Bakkenist and Kastan, 2003; Kozlov et al., 2006). In a reconstituted in vitro system, however, evidence suggests that ATM monomerization by MRN does not

J.A. Daniel and M. Pellegrini contributed equally to this paper.

Correspondence to André Nussenzweig: andre_nussenzweig@nih.gov

Abbreviations used in this paper: ATM, ataxia telangiectasia mutated; BAC, bacterial artificial chromosome; CSR, class switch recombination; DSB, double-strand break; LN, lymph node; LPS, lipopolysaccharide; MRN, MRE11–RAD50–NBS1; PE, phycoerythrin; SP, single positive; TCR, T cell receptor; Tg, transgene; WT, wild type.

This article is distributed under the terms of an Attribution–Noncommercial–Share Alike–No Mirror Sites license for the first six months after the publication date (see <http://www.jcb.org/misc/terms.shtml>). After six months it is available under a Creative Commons License (Attribution–Noncommercial–Share Alike 3.0 Unported license, as described at <http://creativecommons.org/licenses/by-nc-sa/3.0/>).

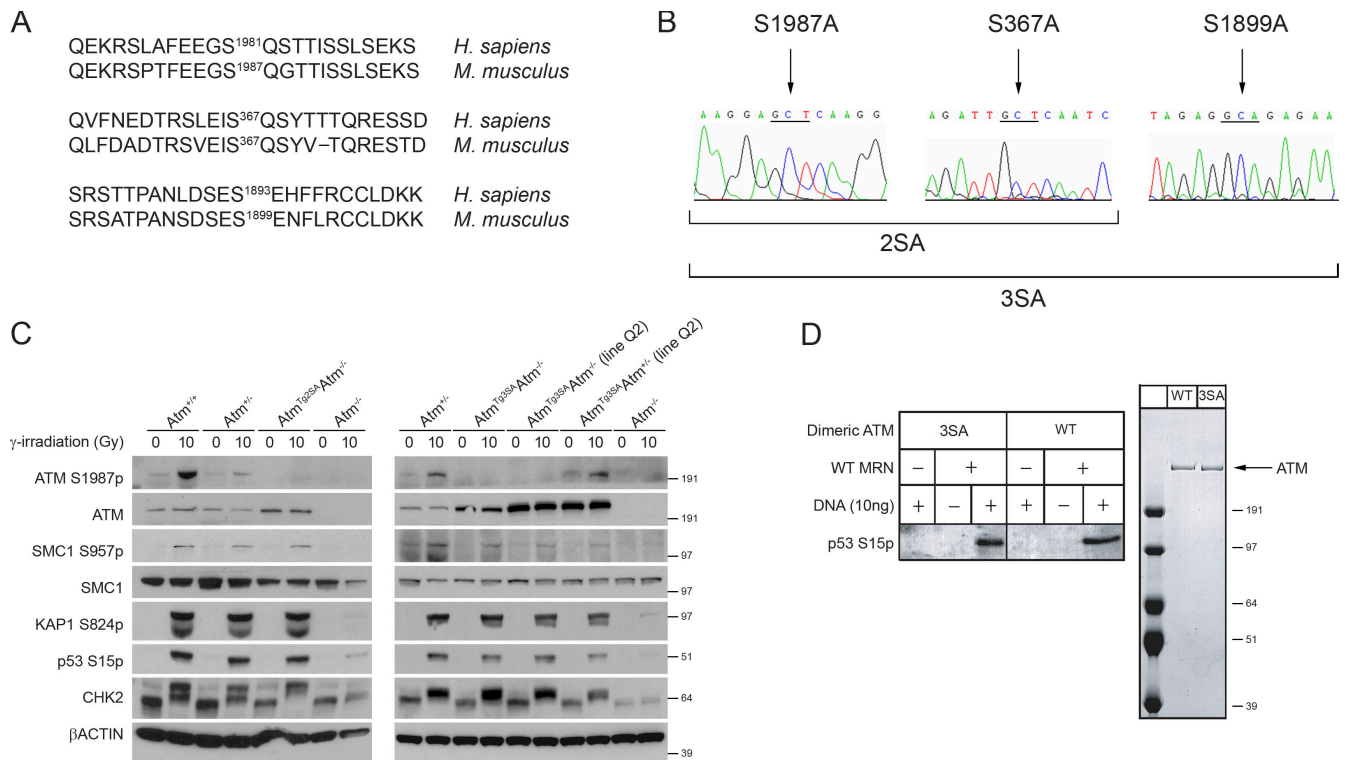


Figure 1. Triple S1987/367/1899A mutant ATM displays normal kinase activity in response to DNA DSBs. (A) Pairwise local alignments of human (*Homo sapiens*) and mouse (*Mus musculus*) ATM protein sequences surrounding sites of autophosphorylation. (B) Sequence chromatograms showing the serine to alanine mutations generated in mouse BAC RP24-122F10. 2SA and 3SA indicate the double serine and triple serine constructs used to generate ATM transgenic mice. (C) B cells stimulated with LPS for 48 h were harvested for lysate preparation and Western blot analysis 30 min after no treatment (0 Gy) or after γ irradiation (10 Gy). Both the 2SA and 3SA mutant ATM proteins expressed ~ 2.5 -fold higher than endogenous levels in *Atm*^{+/+} mice. Line Q2 denotes a different 3SA mutant founder line that expresses mutant ATM ~ 14 -fold higher than endogenous levels in *Atm*^{+/+} mice. (D) Kinase assays with 0.2 nM WT or 3SA mutant dimeric human ATM, 3.6 nM MRN, 50 nM GST-p53 substrate, and linear DNA probed with antibody to p53 S15 phosphorylation. Coomassie blue-stained gel of WT and 3SA mutant dimeric Flag-ATM-HA-ATM complexes. The numbers to the right of the blots represent the measurements in kilodaltons.

require ATM S1981 autophosphorylation (Lee and Paull, 2005). Moreover, using *Xenopus laevis* egg extracts, high concentrations of damaged DNA can promote ATM monomerization without concomitant autophosphorylation (Dupre et al., 2006). Also, in a *Xenopus* system, there is evidence that ATM recruitment to DSBs can precede autophosphorylation (You et al., 2005), further questioning its importance in ATM activation. Because of the lack of physiologically relevant models, the significance of these autophosphorylation sites still remains poorly understood.

Using an ATM transgenic mouse model, we recently found that the most prominent S1981 autophosphorylation site in humans (S1987 in mice) is dispensable for murine ATM function in vivo (Pellegrini et al., 2006). To test whether other putative autophosphorylation sites compensate for the loss of murine S1987, we used bacterial artificial chromosome (BAC) recombineering to generate a transgenic mouse model in which all three conserved ATM serine autophosphorylation sites (S367/1899/1987) have been replaced with alanine. In this study, we show that ATM-dependent responses remain functionally intact in mice that express a double or triple serine mutant form of ATM as their sole ATM species. Collectively, our data strongly support the notion that DNA damage-induced activation of the ATM kinase does not depend on autophosphorylation.

Results and discussion

Triple S1987/367/1899A mutant ATM displays normal kinase activity in response to DNA DSBs

All three human ATM autophosphorylation sites are conserved in the mouse (Fig. 1 A). Using BAC recombineering, we generated double S1987/367A mutant (2SA) ATM mice by creating a second S367A mutation in the S1987A murine ATM BAC described previously (Fig. 1 B; Pellegrini et al., 2006). Subsequently, a third mutation was introduced into the 2SA mutant BAC to change S1899 to alanine and was used to generate triple S1987/367/1899A mutant (3SA) ATM mice (Fig. 1 B). All serine mutation sites were confirmed by sequencing before the generation of transgenic mice (Fig. 1 B). Founder lines expressing mutant ATM from the BAC transgene (Tg) were identified and bred to *Atm*^{+/-} for two generations to obtain *Atm*^{Tg}*Atm*^{-/-} mice. Founder lines A7 and Q7 of *Atm*^{Tg2SA}*Atm*^{-/-} and *Atm*^{Tg3SA}*Atm*^{-/-} mice, respectively, were found to express ATM protein near the level observed in *Atm*^{+/+} mice, whereas another 3SA mutant founder (line Q2) overexpressed ATM protein (Fig. 1 C). All three serine mutations were confirmed in vivo by sequencing 3SA mutant founder Q7 transgenic mouse tail DNA (unpublished data). The A7 and Q7 founder lines were analyzed in detail.

To investigate the role of these autophosphorylation sites in the activation of the ATM kinase, ATM-dependent phosphorylation events were assessed in lysates from cultured splenic B cells irradiated with 10 Gy. As expected, an antibody directed against ATM S1987 autophosphorylation did not recognize ATM in *Atm*^{Tg2SA}*Atm*^{-/-} or *Atm*^{Tg3SA}*Atm*^{-/-} mice, reconfirming the original S1987A mutation in vivo (Fig. 1 C). Splenic B cells from *Atm*^{Tg2SA}*Atm*^{-/-} and *Atm*^{Tg3SA}*Atm*^{-/-} mice responded to γ irradiation similarly to *Atm*^{+/+} and *Atm*^{+/-} by displaying irradiation-induced phosphorylation of SMC1, KAP1, p53, and CHK2 (Fig. 1 C), which are events largely dependent on the ATM kinase (Banin et al., 1998; Canman et al., 1998; Matsuoka et al., 1998; Chaturvedi et al., 1999; Kim et al., 2002; Yazdi et al., 2002; Ziv et al., 2006). Another 3SA mutant founder (line Q2), which overexpressed ATM, also displayed similar irradiation-induced substrate phosphorylation (Fig. 1 C). Similar results were found in thymocytes (unpublished data). Moreover, no differences were found in *Atm*^{Tg3SA}*Atm*^{+/-} transgenic mutants with one wild-type (WT) allele of *Atm* (Fig. 1 C and not depicted), arguing against a predicted dominant interfering activity (Bakkenist and Kastan, 2003; Pellegrini et al., 2006). Together, these results demonstrate that disruption of all three autophosphorylation sites does not affect DNA damage-induced ATM kinase activity in vivo.

To complement our findings in primary mouse cells, we also tested whether all three autophosphorylation sites are required for ATM kinase activity in a completely reconstituted system. WT and 3SA mutant dimeric human ATM complexes were purified by sequential anti-Flag and anti-HA immunoprecipitation, and kinase assays were performed using p53 as a substrate (Lee and Paull, 2005). Consistent with previous findings that mutation of S1981 does not affect monomerization of ATM dimers or kinase activity (Lee and Paull, 2005), 3SA mutant ATM dimers also displayed kinase activity for p53 S15 in an MRN- and DNA-dependent manner similar to WT ATM dimers (Fig. 1 D). Collectively, our data suggest that autophosphorylation events at the conserved S1987, 367, and 1899 sites are dispensable for the kinase activity of ATM in response to DNA breaks.

Triple S1987/367/1899A mutant *Atm* mice display irradiation-induced chromatin retention, cell cycle checkpoint activation, and genomic stability

Evidence for the requirement of S1981 autophosphorylation in the accumulation of ATM at DSB sites is controversial (You et al., 2005; Pellegrini et al., 2006; Berkovich et al., 2007). In this study, using a biochemical method to detect chromatin retention of ATM protein after DNA damage (Andegeko et al., 2001), we found that mutant ATM from *Atm*^{Tg3SA}*Atm*^{-/-} B cells accumulates onto chromatin after 10-Gy irradiation similarly to that from *Atm*^{+/+} (Fig. 2 A). These results demonstrate that autophosphorylation at these three sites is dispensable for ATM retention on damaged chromatin.

However, autophosphorylation could still play a role in downstream functions, including checkpoint activation and maintaining genomic stability. To test whether multiple autophosphory-

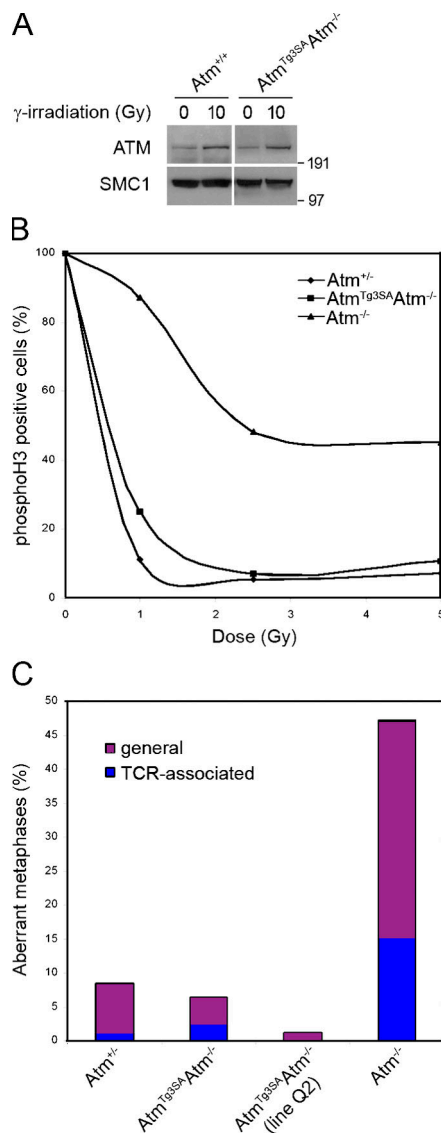


Figure 2. Triple S1987/367/1899A mutant *Atm* mice display normal irradiation-induced chromatin retention, cell cycle checkpoint activation, and genomic stability. (A) B cells stimulated with LPS for 48 h were harvested 30 min after no treatment (0 Gy) or after γ irradiation (10 Gy) and processed for detergent fractionation and Western blot analysis. The numbers to the right of the blot represent the measurements in kilodaltons. (B) B cells stimulated with LPS for 48 h were harvested 1 h after no treatment (unirradiated controls) or after the indicated doses of γ irradiation (grays), and mitotic cells positive for histone H3 S10 phosphorylation were quantified by flow cytometry. Data are normalized with respect to the number of mitotic cells in unirradiated samples from the same genotype. (C) LN T cells stimulated with anti-CD28 + anti-TCR- β for 48 h were treated with colcemid for 1 h and harvested for metaphase chromosome preparation. FISH was performed on slides with probes for TCR-C- α , chromosome 14, and telomeres and counterstained with DAPI. The percentages of metaphases ($n = 80$ for each genotype) with abnormalities specifically associated with the TCR locus on chromosome 14 (TCR associated) or with all other chromosomes (general) are shown.

lation sites are important for checkpoint activation, we irradiated B cells with 0, 1, 2.5, or 5 Gy and assessed the DNA damage-induced G2/M checkpoint by quantifying histone H3 S10 phosphorylation-positive cells containing diploid DNA content. Compared with *Atm*^{-/-}, which displays a defect in the G2/M checkpoint after treatment with ionizing radiation, B cells from

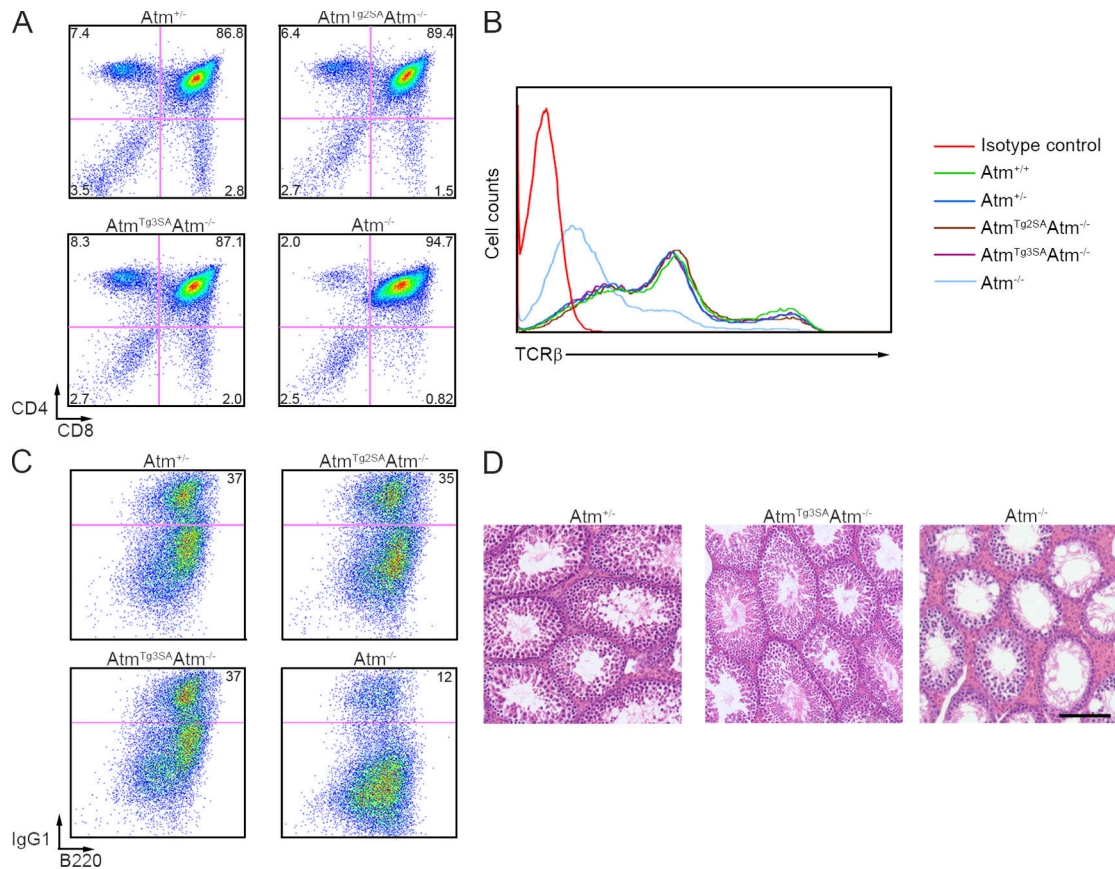


Figure 3. Triple S1987/367/1899A mutant *Atm* mice display normal lymphocyte and germ cell development. (A and B) Freshly isolated thymocytes were harvested and stained to assess cell surface expression of CD4 versus CD8 (A) as well as TCR-β (B) by flow cytometry. (C) B cells stimulated with LPS + IL4 for 96 h were harvested and stained for cell surface markers to assess efficiency of isotype switching to IgG1 by flow cytometry. (D) Hematoxylin and eosin–stained sections of testes from 6-wk-old littermates. (A and C) The numbers represent the percentage of cells in the respective quadrants. Bar, 100 μm.

Atm^{Tg3SA}*Atm*^{-/-} were virtually indistinguishable from those of *Atm*^{+/-} mice (Fig. 2 B). These data suggest that cell cycle checkpoint functions of ATM during the G2/M transition do not require autophosphorylation at S1987, S367, and S1899.

Lymphocytes from ATM-deficient patients and mice display general genomic instability as well as instability at the antigen receptor gene loci caused by aberrant V(D)J recombination (Xu, 1999; Callen et al., 2007b), a gene rearrangement process occurring in developing lymphocytes that increases the antibody repertoire of an individual for defense against pathogens. Characteristic translocations in mature T cells involving the T cell receptor (TCR) locus may contribute to the neoplastic transformation in lymphoid organs of ATM-deficient individuals (Matei et al., 2006; Callen et al., 2007a). To test the role of ATM autophosphorylation in preventing genomic instability, metaphases from *Atm*^{+/-}, *Atm*^{Tg3SA}*Atm*^{-/-}, and *Atm*^{-/-} lymph node (LN) T cells were analyzed for chromosome abnormalities. Compared with *Atm*^{-/-}, in which 32% of the metaphases displayed spontaneous chromosomal aberrations along with an additional 15% associated with the TCR locus, T cells from *Atm*^{Tg3SA}*Atm*^{-/-} mice displayed aberrant metaphases similar to *Atm*^{+/-} (Fig. 2 C). These data strongly suggest that autophosphorylation at S1987, S367, and S1899 are dispensable for the function of ATM in maintaining genomic stability.

Triple S1987/367/1899A mutant *Atm* mice display normal physiological responses during recombination and exposure to ionizing radiation

In the developing thymus, ATM functions in TCR-α gene rearrangement by facilitating the resolution of recombination activation gene–induced DSBs to promote TCR-αβ surface expression for subsequent CD4 and CD8 single-positive (SP) thymocyte selection (Matei et al., 2006; Huang et al., 2007; Vacchio et al., 2007). To begin examining the physiological role of multiple ATM autophosphorylation sites, we performed flow cytometry on freshly isolated thymocytes from *Atm*^{+/+}, *Atm*^{+/-}, *Atm*^{Tg2SA}*Atm*^{-/-}, *Atm*^{Tg3SA}*Atm*^{-/-}, and *Atm*^{-/-} mice to assess thymocyte development. Percentages of CD4 and CD8 SP thymocytes in *Atm*^{Tg2SA}*Atm*^{-/-} and *Atm*^{Tg3SA}*Atm*^{-/-} mice were comparable with those found in *Atm*^{+/-} mice, whereas thymocytes from *Atm*^{-/-} mice showed characteristic reductions in both SP compartments (Fig. 3 A). Moreover, thymocytes from both *Atm*^{Tg2SA}*Atm*^{-/-} and *Atm*^{Tg3SA}*Atm*^{-/-} mice displayed normal distributions of TCR-β surface expression, whereas *Atm*^{-/-} thymocytes showed only low levels (Fig. 3 B), indicating that mice mutant for ATM autophosphorylation sites S1987, S367, and S1899 maintain competency for TCR-α rearrangement and thymocyte development.

A separate antigen receptor gene rearrangement process called class switch recombination (CSR) confers different effector functions for antibodies during an immune response (Stavnezer et al., 2008). In mature B lymphocytes undergoing class switching, ATM functions in recombination of switch regions that lie upstream of the immunoglobulin heavy chain constant region genes (Lumsden et al., 2004; Reina-San-Martin et al., 2004). To further understand the physiological role of multiple autophosphorylation sites for ATM function, we stimulated B cells to undergo CSR at the γ -1 constant region locus. Although *Atm*^{-/-} mice displayed a reduction in IgG1-positive cells (Lumsden et al., 2004; Reina-San-Martin et al., 2004), B cells from both *Atm*^{Tg2SA}*Atm*^{-/-} and *Atm*^{Tg3SA}*Atm*^{-/-} mice exhibited levels of IgG1 switching similar to *Atm*^{+/-} (Fig. 3 C). These results suggest that ATM activation and function during CSR is intact in the absence of S1987, S367, and S1899 autophosphorylation.

The infertility of both male and female *Atm*^{-/-} mice results from a lack of mature gametes caused by chromosomal fragmentation and arrest during meiosis (Barlow et al., 1996; Elson et al., 1996; Xu et al., 1996). *Atm*^{Tg3SA}*Atm*^{-/-} mice had normal testes size and numbers of spermatids within the seminiferous tubules compared with the degeneration and complete absence of spermatids in *Atm*^{-/-} testes (Fig. 3 D). Similar results were obtained from ovaries of *Atm*^{Tg3SA}*Atm*^{-/-} mice (unpublished data). Thus, spermatogenesis and oogenesis disrupted in *Atm*^{-/-} mice appear to be normal in *Atm*^{Tg3SA}*Atm*^{-/-} mice. Collectively, our results demonstrate that physiological DNA rearrangements that require ATM function to resolve DSBs during V(D)J, CSR, and meiotic recombination are not dependent on ATM autophosphorylation at S1987, S367, and S1899.

A hallmark of ataxia telangiectasia is extreme sensitivity to the effects of ionizing radiation (Taylor and Byrd, 2005). Upon radiation exposure, the death of *Atm*^{-/-} mice results from acute radiation toxicity to the gastrointestinal tract (Barlow et al., 1996). To further investigate whether multiple ATM autophosphorylation sites are important for ATM function in vivo, mice were subjected to 8 Gy of whole-body γ irradiation. Intestinal tissues were histologically examined 4 d after irradiation. Recovery from irradiation in the small intestines was similar in *Atm*^{+/-}, *Atm*^{Tg3SA}*Atm*^{-/-}, and *Atm*^{Tg3SA}*Atm*^{+/-} mice, whereas *Atm*^{-/-} mice displayed characteristic toxicity indicated by severe epithelial crypt degeneration and loss of villi (Fig. 4). Examination of the large intestines yielded similar results (unpublished data). These data indicate that ATM autophosphorylation at S1987, S367, and S1899 are not essential for ATM function in vivo to promote tissue recovery after exposure to ionizing radiation.

The differences among results of ATM autophosphorylation mutants, mostly from human cell culture and reconstituted in vitro systems, underscore the necessity for appropriate animal models to ascertain the physiological relevance of ATM post-translational modifications. Although the possibility of different requirements in humans and mice exists, high conservation of the ATM protein sequence between the two organisms as well as the conservation of other phosphatidylinositol-3 kinase-related kinase family members strongly suggests mechanistic similarity in their response to DNA damage (Shiloh, 2003).

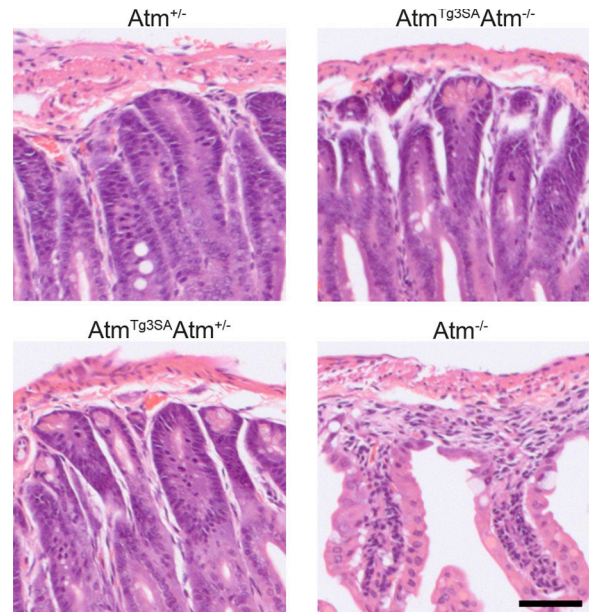


Figure 4. Triple S1987/367/1899A mutant *Atm* mice do not display sensitivity to ionizing radiation. Hematoxylin and eosin–stained sections of small intestines from 8-wk-old littermates 4 d after a dose of 8 Gy whole-body irradiation. Bar, 50 μ m.

Of note, no autophosphorylation site mutations have been identified in ataxia telangiectasia patients described thus far (<http://chromium.liacs.nl/LOVD2/home.php>).

Our results from transgenic mouse models strongly suggest that ATM autophosphorylation at S1987, S367, and S1899 is dispensable for the DNA damage–induced activation and function of the kinase in vivo. We show that 3SA autophosphorylation mutant ATM can accumulate at sites of DNA damage, phosphorylate target substrates, activate cell cycle checkpoints, maintain genomic stability, and function in lymphocyte and meiotic recombination processes as well as in the recovery from whole-body irradiation. Because expression of the mutant ATM protein is 2.5-fold higher than normal, it is possible that this could mask a nonessential role for ATM autophosphorylation on ATM activity. For example, if ATM autophosphorylation were to enhance ATM activity 2.5-fold and the nonphosphorylatable ATM were expressed 2.5-fold higher than normal, mice expressing the Tg might be normal in terms of ATM function. This seems unlikely because levels of ATM expressed over a range of one- to sixfold higher than normal in *Atm*^{TgWT} and *Atm*^{TgS1987A} mice (Pellegrini et al., 2006) display indistinguishable ATM substrate phosphorylations compared with *Atm*^{+/-} and *Atm*^{+/+} controls. Moreover, TgWT, TgS1987A, Tg2SA, and Tg3SA completely rescue the defects in growth, lymphocyte development, and meiotic arrest observed in *Atm*^{-/-} mice (Pellegrini et al., 2006). On a different note, at least three other ATM phosphorylation sites have been identified in response to DNA damage besides S367, S1893, and S1981 (Kozlov et al., 2006; Matsuoka et al., 2007), some of which may also be sites of autophosphorylation, raising the formal possibility that other autophosphorylation sites may still compensate for the loss of S1987/367/1899. Nevertheless, pretreatment of human cells in culture with the KU55933 ATM kinase inhibitor did not

affect the irradiation-induced increase in ATM kinase activity (Pellegrini et al., 2006), providing additional evidence against an essential role for autophosphorylation in ATM activation.

Collectively with our *in vivo* evidence, we propose that ATM autophosphorylation occurs simultaneously or as a consequence of ATM activation and may be the combined result of ATM localization to break sites along with promiscuous phosphorylation of consensus sites exposed on the surface of ATM. By proposing that autophosphorylation is not the mechanism of ATM activation, we stimulate speculation on the relevant way in which damaged chromatin activates the ATM kinase. The MRN complex clearly plays a critical role in ATM activation by retaining ATM to DNA breaks, stimulating substrate binding, and directly stimulating kinase activity through activities on DNA by the RAD50 ATPase (Lee and Paull, 2007). Growing evidence suggests that ATM activation at DNA damage sites is mediated through direct recruitment by MRN, and to what extent other posttranslational modifications of ATM, such as acetylation at lysine 3016 (Sun et al., 2007), may function remains to be determined.

Materials and methods

Generation of mice

The S1987A mutant murine *Atm* BAC (Pellegrini et al., 2006) was recombinered as described previously (Yang and Sharan, 2003) to contain an EcoRI site between exons 35 and 36 for a PCR-based method to distinguish between *Atm*⁹*Atm*^{-/-} and *Atm*⁹*Atm*^{+/-} genotypes. The S367A and S1899A mutations were sequentially targeted into the S1987A EcoRI site-containing BAC as described previously (Yang and Sharan, 2003), and both double serine and triple serine mutant BACs were used to generate transgenic mice. The presence of the Tg was determined by PCR as previously described (Pellegrini et al., 2006). Transgenic founders were crossed to *Atm*^{+/-} mice. All experiments were performed with 2SA A7 and 3SA Q7 founder lines unless otherwise noted. All experiments were performed in compliance with the National Institutes of Health Intramural Animal Care and Use program.

Lymphocyte cultures

B cells were isolated from spleens of 6–12-wk-old mice by immunomagnetic depletion with anti-CD43 beads (Miltenyi Biotec) and stimulated with either 25 µg/ml lipopolysaccharide (LPS) alone (Sigma-Aldrich) or in combination with 5 ng/ml interleukin 4 (IL4; Sigma-Aldrich) for 2–4 d as indicated. LN T cells of 6–12-wk-old mice were stimulated with 2 µg/ml anti-TCR-β (H57; BD) and 5 µg/ml anti-CD28 (BD) antibodies for 48 h.

Western blotting

Whole cell lysates were prepared as previously described (Difilippantonio et al., 2005). The association of ATM with chromatin after irradiation was determined using detergent extraction as previously described (Andegeko et al., 2001). Anti-KAP1 S824 phospho (Bethyl Laboratories, Inc.) was used at a 1:2,000 dilution. All other antibodies used for Western blotting were previously described (Lee and Paull, 2005; Pellegrini et al., 2006). Human ATM dimers and/or multimers were purified by sequential anti-Flag and anti-HA immunoprecipitation, and kinase assays were performed as previously described (Lee and Paull, 2005).

Metaphase and G2/M checkpoint analysis

Cultured LN T cells were arrested at mitosis with 0.1 µg/ml colcemid (Roche) treatment for 1 h, and metaphase chromosome spreads were prepared according to standard procedures. FISH was performed on slides with probes for TCR- α (from BAC 232F18), chromosome 14 (a gift from T. Reid, National Cancer Institute, Bethesda, MD), and telomere repeat-specific peptide nucleic acid (Applied Biosystems) and counterstained with DAPI. Images were acquired with an upright microscope (Axioplan2; Carl Zeiss, Inc.) equipped with a 63 \times NA 1.4 objective lens (Plan-Apochromat; Nikon) and a monochrome charge-coupled device camera (Orca ER; Hamamatsu Photonics) using Metamorph software (MDS Analytical

Technologies). G2/M checkpoint assays were performed on stimulated B cells as previously described (Fernandez-Capetillo et al., 2002).

Flow cytometry

Single-cell suspensions of thymocytes were stained with anti-CD4-phycoerythrin (PE), anti-CD8-FITC, or anti-TCR- β -PE (BD). B cells cultured for 4 d were harvested and stained in single-cell suspensions with anti-B220-FITC and anti-IgG1-biotin followed by streptavidin-PE. Cells were acquired with either a FACScan or a FACSCalibur (BD) along with CellQuest software (BD) using a live lymphocyte gate except for a propidium iodide-negative gate used in CSR analysis of B cells. Data were analyzed using FlowJo software (version 7.2.4; Tree Star, Inc.).

Histology

Testes and small intestines were fixed in 10% formalin, and paraffin sections were stained with hematoxylin and eosin. Images were acquired with an inverted microscope (Axiovert 200M; Carl Zeiss, Inc.) equipped with a 10 \times NA 0.45 objective lens (Plan-Apochromat; Nikon) and a color charge-coupled device camera (AxioCam MRC5; Carl Zeiss, Inc.) using AxioVision software (version 4.6.3.0; Carl Zeiss, Inc.).

We thank Steve Jay, Dave Winkler, Michael Kruhlak, Elsa Callén, and Michael Eckhaus for technical assistance, the Thomas Reid laboratory for chromosome 14 paint FISH probe, and Joan Yuan for critical reading of the manuscript.

This work was supported by the Intramural Research Program of the National Institutes of Health, National Cancer Institute, Center for Cancer Research, and the A-T Children's Project.

Submitted: 26 May 2008

Accepted: 30 October 2008

References

- Andegeko, Y., L. Moyal, L. Mittelman, I. Tsarfaty, Y. Shiloh, and G. Rotman. 2001. Nuclear retention of ATM at sites of DNA double strand breaks. *J. Biol. Chem.* 276:38224–38230.
- Bakkenist, C.J., and M.B. Kastan. 2003. DNA damage activates ATM through intermolecular autophosphorylation and dimer dissociation. *Nature.* 421:499–506.
- Banin, S., L. Moyal, S. Shieh, Y. Taya, C.W. Anderson, L. Chessa, N.I. Smorodinsky, C. Prives, Y. Reiss, Y. Shiloh, and Y. Ziv. 1998. Enhanced phosphorylation of p53 by ATM in response to DNA damage. *Science.* 281:1674–1677.
- Barlow, C., S. Hirotsune, R. Paylor, M. Liyanage, M. Eckhaus, F. Collins, Y. Shiloh, J.N. Crawley, T. Ried, D. Tagle, and A. Wynshaw-Boris. 1996. Atm-deficient mice: a paradigm of ataxia telangiectasia. *Cell.* 86:159–171.
- Berkovich, E., R.J. Monnat Jr., and M.B. Kastan. 2007. Roles of ATM and NBS1 in chromatin structure modulation and DNA double-strand break repair. *Nat. Cell Biol.* 9:683–690.
- Bredemeyer, A.L., G.G. Sharma, C.Y. Huang, B.A. Helmkink, L.M. Walker, K.C. Khor, B. Nuskey, K.E. Sullivan, T.K. Pandita, C.H. Bassing, and B.P. Sleckman. 2006. ATM stabilizes DNA double-strand-break complexes during V(D)J recombination. *Nature.* 442:466–470.
- Callen, E., M. Jankovic, S. Difilippantonio, J.A. Daniel, H.T. Chen, A. Celeste, M. Pellegrini, K. McBride, D. Wangsa, A.L. Bredemeyer, et al. 2007a. ATM prevents the persistence and propagation of chromosome breaks in lymphocytes. *Cell.* 130:63–75.
- Callen, E., M.C. Nussenzweig, and A. Nussenzweig. 2007b. Breaking down cell cycle checkpoints and DNA repair during antigen receptor gene assembly. *Oncogene.* 26:7759–7764.
- Canman, C.E., D.S. Lim, K.A. Cimprich, Y. Taya, K. Tamai, K. Sakaguchi, E. Appella, M.B. Kastan, and J.D. Siliciano. 1998. Activation of the ATM kinase by ionizing radiation and phosphorylation of p53. *Science.* 281:1677–1679.
- Carson, C.T., R.A. Schwartz, T.H. Stracker, C.E. Lilley, D.V. Lee, and M.D. Weitzman. 2003. The Mre11 complex is required for ATM activation and the G2/M checkpoint. *EMBO J.* 22:6610–6620.
- Cerosaletti, K., J. Wright, and P. Concannon. 2006. Active role for nibrin in the kinetics of atm activation. *Mol. Cell. Biol.* 26:1691–1699.
- Chaturvedi, P., W.K. Eng, Y. Zhu, M.R. Mattern, R. Mishra, M.R. Hurler, X. Zhang, R.S. Annan, Q. Lu, L.F. Faucette, et al. 1999. Mammalian Chk2 is a downstream effector of the ATM-dependent DNA damage checkpoint pathway. *Oncogene.* 18:4047–4054.
- Difilippantonio, S., A. Celeste, O. Fernandez-Capetillo, H.T. Chen, B. Reina San Martin, F. Van Laethem, Y.P. Yang, G.V. Petukhova, M. Eckhaus, L.

- Feigenbaum, et al. 2005. Role of Nbs1 in the activation of the Atm kinase revealed in humanized mouse models. *Nat. Cell Biol.* 7:675–685.
- Dupre, A., L. Boyer-Chatenet, and J. Gautier. 2006. Two-step activation of ATM by DNA and the Mre11-Rad50-Nbs1 complex. *Nat. Struct. Mol. Biol.* 13:451–457.
- Elson, A., Y. Wang, C.J. Daugherty, C.C. Morton, F. Zhou, J. Campos-Torres, and P. Leder. 1996. Pleiotropic defects in ataxia-telangiectasia protein-deficient mice. *Proc. Natl. Acad. Sci. USA.* 93:13084–13089.
- Fernandez-Capetillo, O., H.T. Chen, A. Celeste, I. Ward, P.J. Romanienko, J.C. Morales, K. Naka, Z. Xia, R.D. Camerini-Otero, N. Motoyama, et al. 2002. DNA damage-induced G2-M checkpoint activation by histone H2AX and 53BP1. *Nat. Cell Biol.* 4:993–997.
- Girard, P.M., E. Riballo, A.C. Begg, A. Waugh, and P.A. Jeggo. 2002. Nbs1 promotes ATM dependent phosphorylation events including those required for G1/S arrest. *Oncogene.* 21:4191–4199.
- Huang, C.Y., G.G. Sharma, L.M. Walker, C.H. Bassing, T.K. Pandita, and B.P. Sleckman. 2007. Defects in coding joint formation in vivo in developing ATM-deficient B and T lymphocytes. *J. Exp. Med.* 204:1371–1381.
- Kim, S.T., B. Xu, and M.B. Kastan. 2002. Involvement of the cohesin protein, Smc1, in Atm-dependent and independent responses to DNA damage. *Genes Dev.* 16:560–570.
- Kozlov, S.V., M.E. Graham, C. Peng, P. Chen, P.J. Robinson, and M.F. Lavin. 2006. Involvement of novel autophosphorylation sites in ATM activation. *EMBO J.* 25:3504–3514.
- Lee, J.H., and T.T. Paull. 2004. Direct activation of the ATM protein kinase by the Mre11/Rad50/Nbs1 complex. *Science.* 304:93–96.
- Lee, J.H., and T.T. Paull. 2005. ATM activation by DNA double-strand breaks through the Mre11-Rad50-Nbs1 complex. *Science.* 308:551–554.
- Lee, J.H., and T.T. Paull. 2007. Activation and regulation of ATM kinase activity in response to DNA double-strand breaks. *Oncogene.* 26:7741–7748.
- Lumsden, J.M., T. McCarty, L.K. Petiniot, R. Shen, C. Barlow, T.A. Wynn, H.C. Morse III, P.J. Gearhart, A. Wynshaw-Boris, E.E. Max, and R.J. Hodes. 2004. Immunoglobulin class switch recombination is impaired in Atm-deficient mice. *J. Exp. Med.* 200:1111–1121.
- Matei, I.R., C.J. Guidos, and J.S. Danska. 2006. ATM-dependent DNA damage surveillance in T-cell development and leukemogenesis: the DSB connection. *Immunol. Rev.* 209:142–158.
- Matsuoka, S., M. Huang, and S.J. Elledge. 1998. Linkage of ATM to cell cycle regulation by the Chk2 protein kinase. *Science.* 282:1893–1897.
- Matsuoka, S., B.A. Ballif, A. Smogorzewska, E.R. McDonald III, K.E. Hurov, J. Luo, C.E. Bakalarski, Z. Zhao, N. Solimini, Y. Lerenthal, et al. 2007. ATM and ATR substrate analysis reveals extensive protein networks responsive to DNA damage. *Science.* 316:1160–1166.
- McKinnon, P.J., and K.W. Caldecott. 2007. DNA strand break repair and human genetic disease. *Annu. Rev. Genomics Hum. Genet.* 8:37–55.
- Pellegrini, M., A. Celeste, S. Difilippantonio, R. Guo, W. Wang, L. Feigenbaum, and A. Nussenzweig. 2006. Autophosphorylation at serine 1987 is dispensable for murine Atm activation in vivo. *Nature.* 443:222–225.
- Reina-San-Martin, B., H.T. Chen, A. Nussenzweig, and M.C. Nussenzweig. 2004. ATM is required for efficient recombination between immunoglobulin switch regions. *J. Exp. Med.* 200:1103–1110.
- Shiloh, Y. 2003. ATM and related protein kinases: safeguarding genome integrity. *Nat. Rev. Cancer.* 3:155–168.
- Stavnezer, J., J.E. Guikema, and C.E. Schrader. 2008. Mechanism and regulation of class switch recombination. *Annu. Rev. Immunol.* 26:261–292.
- Sun, Y., Y. Xu, K. Roy, and B.D. Price. 2007. DNA damage-induced acetylation of lysine 3016 of ATM activates ATM kinase activity. *Mol. Cell. Biol.* 27:8502–8509.
- Taylor, A.M., and P.J. Byrd. 2005. Molecular pathology of ataxia telangiectasia. *J. Clin. Pathol.* 58:1009–1015.
- Uziel, T., Y. Lerenthal, L. Moyal, Y. Andegeko, L. Mittelman, and Y. Shiloh. 2003. Requirement of the MRN complex for ATM activation by DNA damage. *EMBO J.* 22:5612–5621.
- Vacchio, M.S., A. Orlar, F. Livak, and R.J. Hodes. 2007. ATM deficiency impairs thymocyte maturation because of defective resolution of T cell receptor alpha locus coding end breaks. *Proc. Natl. Acad. Sci. USA.* 104:6323–6328.
- Xu, Y. 1999. ATM in lymphoid development and tumorigenesis. *Adv. Immunol.* 72:179–189.
- Xu, Y., T. Ashley, E.E. Brainerd, R.T. Bronson, M.S. Meyn, and D. Baltimore. 1996. Targeted disruption of ATM leads to growth retardation, chromosomal fragmentation during meiosis, immune defects, and thymic lymphoma. *Genes Dev.* 10:2411–2422.
- Yang, Y., and S.K. Sharan. 2003. A simple two-step, ‘hit and fix’ method to generate subtle mutations in BACs using short denatured PCR fragments. *Nucleic Acids Res.* 31:e80.
- Yazdi, P.T., Y. Wang, S. Zhao, N. Patel, E.Y. Lee, and J. Qin. 2002. SMC1 is a downstream effector in the ATM/NBS1 branch of the human S-phase checkpoint. *Genes Dev.* 16:571–582.
- You, Z., C. Chahwan, J. Bailis, T. Hunter, and P. Russell. 2005. ATM activation and its recruitment to damaged DNA require binding to the C terminus of Nbs1. *Mol. Cell. Biol.* 25:5363–5379.
- You, Z., J.M. Bailis, S.A. Johnson, S.M. Dilworth, and T. Hunter. 2007. Rapid activation of ATM on DNA flanking double-strand breaks. *Nat. Cell Biol.* 9:1311–1318.
- Ziv, Y., D. Bielopolski, Y. Galanty, C. Lukas, Y. Taya, D.C. Schultz, J. Lukas, S. Bekker-Jensen, J. Bartek, and Y. Shiloh. 2006. Chromatin relaxation in response to DNA double-strand breaks is modulated by a novel ATM- and KAP-1 dependent pathway. *Nat. Cell Biol.* 8:870–876.